Pergamon

Calphad Vol. 23, No. 2, pp. 219–230, 1999

0364-5916/99/$ - see front matter

PII: S0364-5916(99)00026-7

MODELING THE CHARGE COMPENSATION EFFECT IN SILICA-RICH Na_2O-K_2O-Al_2O_3-SiO_2 MELTS

Patrice Chartrand and Arthur D. Pelton
Centre de Recherche en Calcul Thermochimique
École Polytechnique de Montréal
P. O. Box 6079, Station "Downtown"
Montreal, Québec H3C 3A7
Canada

(Presented at CALPHAD XXVIII, Grenoble, France, May 1999)

ABSTRACT At high SiO_2 contents, a model of Na_2O-K_2O-Al_2O_3-SiO_2 melts must take into account the "charge compensation effect" whereby the replacement of a tetravalent Si^{4+} by a trivalent Al^{3+} in the silicate network is facilitated by the formation of $(NaAl)^{4+}$ or $(KAl)^{4+}$ associates. This effect has been taken into account in the quasichemical model by treating the $(NaAl)^{4+}$ and $(KAl)^{4+}$ associates as separate species in the melt, which is then formally treated as consisting of the components $NaO_{1/2}$, $KO_{1/2}$, $AlO_{3/2}$, SiO_2, $(NaAl)O_2$ and $(KAl)O_2$. Optimizations of the Na_2O-Al_2O_3-SiO_2, K_2O-Al_2O_3-SiO_2 and $NaAlSiO_4$-$KAlSiO_4$-SiO_2 systems at high SiO_2 contents are reported.

1. INTRODUCTION

Over the past several years we have used the modified quasichemical model [1-3] for the optimization of a large number of multicomponent molten oxide solutions. This model treats short-range ordering in the pair approximation. For example, for a solution AO_x-BO_y-SiO_2 (such as $NaO_{1/2}$-$AlO_{3/2}$-SiO_2), the parameters of the model are the Gibbs energies of formation of second-nearest-neighbour pairs according to:

$$(A-A)+(Si-Si)=2(A-Si); \qquad \Delta g^o_{ASi}=\omega_{ASi}-\eta_{ASi}T \tag{1}$$

$$(B-B)+(Si-Si)=2(B-Si); \qquad \Delta g^o_{BSi}=\omega_{BSi}-\eta_{BSi}T \tag{2}$$

$$(A-A)+(B-B)=2(A-B); \qquad \Delta g^o_{AB}=\omega_{AB}-\eta_{AB}T \tag{3}$$

where (X-Y) represents a second-nearest-neighbour pair. For example, (Si-Si) represents a pair of network silicons joined by a "bridging" oxygen: (Si-O-Si). The Gibbs energy of the solution is given by:

$$G=\left(n_{AO_x}g^o_{AO_x}+n_{BO_y}g^o_{BOy}+n_{SiO_2}g^o_{SiO_2}\right)-T\Delta S^{config} +\left(n_{ASi}\Delta g^o_{ASi}+n_{BSi}g^o_{BSi}+n_{AB}\Delta g^o_{AB}\right) \tag{4}$$

where n_i and Δg_i^o are the number of moles and standard molar Gibbs energy of component i (i=AO_x, BO_y, SiO_2); n_{xy} is the number of moles of second-nearest-neighbour (X-Y) pairs; and ΔS^{config} is the configurational entropy which is given by the following (Ising) approximation for the random distribution of the pairs over "pair positions" :

Received on 23 April 1999

$$\Delta S^{config} = -R\left(n_{AO_x}\ln X_{AO_x} + n_{BO_y}\ln X_{BO_y} + n_{SiO_2}\ln X_{SiO_2}\right)$$
$$-R\left[n_{AA}\ln\frac{X_{AA}}{Y_A^2} + n_{BB}\ln\frac{X_{BB}}{Y_B^2} + n_{SiSi}\ln\frac{X_{SiSi}}{Y_{Si}^2}\right. \quad (5)$$
$$\left. + n_{ASi}\ln\frac{X_{ASi}}{2Y_AY_{Si}} + n_{BSi}\ln\frac{X_{BSi}}{2Y_BY_{Si}} + n_{AB}\ln\frac{X_{AB}}{2Y_AY_B}\right]$$

where X_i is the mole fraction of component i, X_{XY} is the bond fraction of (X-Y) bonds:

$$X_{XY} = n_{XY} / \sum n_{ij} \quad (6)$$

and Y_A, Y_B and Y_{Si} are "equivalent fractions" given by:

$$Y_A = \frac{Z_A X_{AO_x}}{Z_A X_{AO_x} + Z_B X_{BO_y} + Z_{Si} X_{SiO_2}} \quad (7)$$

where Z_i is the second-nearest-neighbour "coordination number" of i.

The equilibrium state is computed by minimizing G subject to the mass balance constraints [1-3].

In a binary system, such as $NaO_{1/2}$-SiO_2, if the parameter Δg^o_{NaSi} (see eq. 1) is very negative then (Na-Si) pairs will predominate, and both the enthalpy and entropy will exhibit minima near the composition $Y_{Na} = Y_{Si} = 0.5$. The corresponding mole fractions are determined by the ratio (Z_{Si}/Z_{Na}). By setting this ratio equal to 4.0, we set the composition of maximum short-range ordering at $X_{NaO_{1/2}} = 0.8$, which is the orthosilicate composition, Na_4SiO_4. Since the expression for ΔS^{config} in Eq. (5) is an approximation, the values of Z_i which yield the best optimizations do not necessarily correspond to the actual coordination numbers (although their ratios correspond to the actual ratios). As discussed previously [1-3], the appropriate values for $NaO_{1/2}$, $AlO_{3/2}$, and SiO_2 are: $Z_{Si} = (4\ Z_{Na}) = (4/3\ Z_{Al}) = 2.7548$.

For purposes of optimization of experimental data, the Δg^o_{ij} parameters are expressed as empirical power series in the equivalent fractions [1-3]. For example, the optimization of the $NaO_{1/2}$-SiO_2 binary system [4] gives the following optimized expression for the liquid:

$$\Delta g^\circ_{NaSi} = -114345 + 43.932\,T - 381598\,Y_{Si} + (123010 + 20.920\,T)\,Y_{Si}^7 \quad J/mol \quad (8)$$

The optimized phase diagram is compared with several experimental data points [5-8] in Fig. 1. Experimental activities in the liquid are also closely reproduced. Details of the optimization, as well as expressions for the standard molar Gibbs energies of all compounds, have been given previously [4]. Note that, as expected, Δg^o_{NaSi} is very negative in this binary system, reflecting the strong tendency of the "network modifier", Na_2O, to break the (Si-O-Si) bridges and form stable ordered solutions.

By contrast, the optimization [9] of the $AlO_{3/2}$-SiO_2 system gave the following optimized expression for the liquid:

$$\Delta g^\circ_{AlSi} = 4800 + 100784\,Y_{Si}^3 - 142068\,Y_{Si}^5 + 78571\,Y_{Si}^7 \quad J/mol \quad (9)$$

In this system, Δg^o_{AlSi} is slightly positive. Liquid $AlO_{3/2}$-SiO_2 solutions exhibit slight positive deviations from ideality. The optimized phase diagram is compared with some experimental data points [10, 11] in Fig. 2. Full details of the optimizations and values of standard Gibbs energies of all compounds have been given previously [9].

A similar optimization of the Na_2O-Al_2O_3 system has been performed [12]. Using these three binary optimizations, Wu [12] used Eq. (4) to estimate G of ternary liquid $NaO_{1/2}$-$AlO_{3/2}$-SiO_2 solutions, and then used this estimate to calculate the ternary liquidus surface. In these calculations the

asymmetric approximation [2,3] was used; that is, it was assumed that Δg^{o}_{NaSi} and Δg^{o}_{AlSi} in Eq. (4) in the ternary solution are constant along lines of constant Y_{Si}, such that Eqs. (8) and (9) may be substituted directly into Eq. (4), while Δg^{o}_{NaAl} was assumed to be constant along lines of constant ratio (Y_{Na}/Y_{Al}).

The ternary liquidus surface calculated in this way is in very poor agreement with the experimental phase diagram. In order to improve the agreement, Wu [12] included several empirical "ternary parameters". These account for the influence of the third component upon the Gibbs energies of formation Δg^{o}_{ij} of the binary pairs. For example, the effect of Al upon Δg^{o}_{NaSi} is modeled by adding terms such as $\omega^{ij}_{NaSi(Al)} Y^{i}_{Si} (Y_{Al}/(Y_{Al}+Y_{Na}))^{j}$ to Eq. (8), where $\omega^{ij}_{NaSi(Al)} (j \neq 0)$ is an empirical ternary parameter obtained from the optimization of ternary data.s

Even with 5 large ternary parameters, Wu was unable to obtain a satisfactory representation of the ternary liquidus. This result is in contrast to our finding that, in many other ternary and multicomponent systems involving the components SiO_2-Al_2O_3-CaO-MgO-FeO-Fe_2O_3-PbO-ZnO-CrO-Cr_2O_3-Cu_2O-etc. [2, 3, 9, 12, 13-19], the quasichemical model gives good approximations of the Gibbs energy of the liquid oxide solutions with only a few small, or with no, ternary parameters.

2. MODELING THE CHARGE COMPENSATION EFFECT

Clearly, the assumptions of the model are inadequate in the case of $NaO_{1/2}$-$AlO_{3/2}$-SiO_2 solutions. An indication of how the model might be improved is provided by two features of the experimental liquidus surface. In Fig. 3a it can be seen that the liquidus of mullite descends very steeply from the SiO_2-Al_2O_3 binary system to the SiO_2-$NaAlO_2$ join [20]. This shows that liquid SiO_2-Al_2O_3 solutions are very strongly stabilized by the addition of Na_2O up to a molar Na:Al ratio of 1:1. The second feature is seen in Fig. 4 which shows the liquidus along SiO_2-$NaAlO_2$ join between SiO_2 and albite, ($NaAlSi_3O_8$). In the limit as $X_{SiO_2} \rightarrow 1$, the limiting slope of the SiO_2-liquidus is given by Raoult's law as:

$$\lim_{X_{SiO_2} \rightarrow 1} \left(dX_{SiO_2}/dT\right) = \Delta h^{o}_{f(SiO_2)} / \nu R T^{2}_{fus(SiO_2)} \qquad (10)$$

where $\Delta h^{o}_{f(SiO_2)}$ and $T_{f(SiO_2)}$ are the enthalpy and temperature of fusion of SiO_2 and ν is the number of moles of independent atoms or ions introduced per mole of $NaAlO_2$ (or of $NaAlSi_3O_8$). The experimental [21] points show that the limiting liquidus slope corresponds closely to $\nu = 1$. That is, Na and Al enter into solution as (NaAl) associates. The simple quasichemical model, however, predicts $\nu = 2$ in the limit as $X_{SiO_2} \rightarrow 1$.. (By setting $\Delta g^{o}_{NaAl} << 0$, the concentration of (Na-Al) nearest-neighbour pairs could, of course, be increased. However, a calculated liquid-liquid miscibility gap would then appear along the $NaAlO_2$-SiO_2 join due to clustering of (Na-Al) and (Si-Si) pairs.)

The above observations are usually interpreted as arising from a "charge compensation effect". The dissolution of alum na in silica by the replacement of a tetravalent silicon in the tetrahedral network by a trivalent aluminum is energetically unfavourable because it results in a negative charge centre. However, upon addition of Na_2O this negative charge can be compensated by a Na^{+} ion placed next to the aluminum as illustrated in Fig. 5. Hence, the addition of Na_2O, up to a Na:Al ratio of 1:1, decreases the Gibbs energy of the solution markedly.

To model this effect, we consider the $(NaAl)^{4+}$ associates to be a separate species. The ternary solution is then formally treated as a quaternary solution with components $NaO_{1/2}$, $AlO_{3/2}$, SiO_2 and $(NaAl)O_2$ where the mole fraction $X_{(NaAl)O_2}$ gives the concentration of the (NaAl) associates, while $X_{NaO_{1/2}}$ and $X_{AlO_{3/2}}$ are the concentrations of "free" Na and Al. The formation of the (NaAl) associates is formally treated through the Gibbs energy change of the following reaction among the components:

$$NaO_{1/2} + AlO_{3/2} = (NaAl)O_2 \tag{11}$$

$$\Delta G^o_{(NaAl)O_2} = g^o_{(NaAl)O_2} - g^o_{NaO_{1/2}} - g^o_{AlO_{3/2}} \tag{12}$$

where $g^o_{(NaAl)O_2}$ is the standard Gibbs energy of the hypothetical pure component $(NaAl)O_2$. In the modified model, this is a parameter which is determined by optimization.

We must now also introduce, as parameters, the Gibbs energies of formation of the following second-nearest-neighbour pairs:

$$(Si-Si)+(NaAl-NaAl) = 2(NaAl-Si); \qquad \Delta g^o_{(NaAl)Si} \tag{13}$$

$$(Al-Al)+(NaAl-NaAl) = 2(NaAl-Al), \qquad \Delta g^o_{g(NaAl)Al} \tag{14}$$

$$(Na-Na)+(NaAl-NaAl) = 2(NaAl-Na); \qquad \Delta g^o_{(NaAl)Na} \tag{15}$$

(One must clearly distinguish an (NaAl) associate from an (Na-Al) pair, the latter being a second-nearest-neighbour pair between a "free" Na and "free" Al.).

The Gibbs energy of the solution is then given by a 4-component quasichemical expression (like Eq. (4) but with a fourth component, CO_2), where ΔS^{config} is given by randomly distributing all types of pairs: (Na-Na), (Al-Al), (Si-Si) (NaAl-NaAl), (Na-Al), (Na-Si), (NaAl-Na), (Al-Si), (NaAl-Al), and (NaAl-Si). Minimizing G subject to the mass balance constraints then gives all the equilibrium bond fractions as well as the equilibrium mole fraction of associates, $X_{(NaAl)O_2}$

2-1. The Na_2O-Al_2O_3-SiO_2 system

The Na_2O-Al_2O_3-SiO_2 system was optimized with the modified model. The coordination number $Z_{(NaAl)}$ was set equal to $Z_{Si} = 2.7548$. The expressions for Δg^o_{NaSi} and Δg^o_{AlSi} were taken from the binary optimizations, Eqs. (8,9). The parameters Δg^o_{NaAl}, $\Delta g^o_{(NaAl)Na}$ and $\Delta g^o_{(NaAl)Al}$ were all set to zero. The following optimized expressions were then obtained for $\Delta G^o_{(NaAl)O_2}$ and $\Delta g^o_{(NaAl)Si}$, both of which have large negative values:

$$\Delta G^o_{(NaAl)O_2} = -146440 \quad J/mol \tag{16}$$

$$\Delta g^o_{(NaAl)Si} = -44750 + 16.736\,T - 10479\,Y_{Si} - 4184\left(Y_{Al}/\left(Y_{Na}+Y_{Al}+Y_{(NaAl)}\right)\right) \quad J/mol \tag{17}$$

The standard Gibbs energies of all components and binary compounds were given previously [4, 9]. For albite ($NaAlSi_3O_8$), the standard Gibbs energy, shown in Table 1, was taken from the literature [22, 23].

The calculated liquidus surface is shown in Fig. 3b, which may be compared to the experimental [20] phase diagram in Fig. 3a. Calculations along the $NaAlSi_3O_8$-SiO_2 join and the $NaAlSi_3O_8$-Al_2O_3 join are compared to measurements [21] in Figs. 4 and 6 respectively. It should be noted that the first three terms of Eq. (17) for $\Delta g^o_{(NaAl)Si}$ are "binary" terms for the pseudobinary $(NaAl)O_2$-SiO_2 system, while the final term is a "ternary" term for the $(NaAl)O_2$-$AlO_{3/2}$ – SiO_2 ternary "sub-system". That is, the very good agreement between calculations and measurements was obtained with only one ternary term for this sub-system, and with no ternary terms for the SiO_2-$(NaAl)O_2$-$NaO_{1/2}$ sub-system. (The final term in Eq. (17) has virtually no effect in the SiO_2-$(NaAl)O_2$-$NaO_{1/2}$ sub-system because the equivalent fraction of "free" Al^{3+}, Y_{Al}, is very small in this sub-system.) In particular, the steep mullite liquidus, and the limiting liquidus slope at $X_{SiO_2} = 1$ in Fig. 4 are very well reproduced.

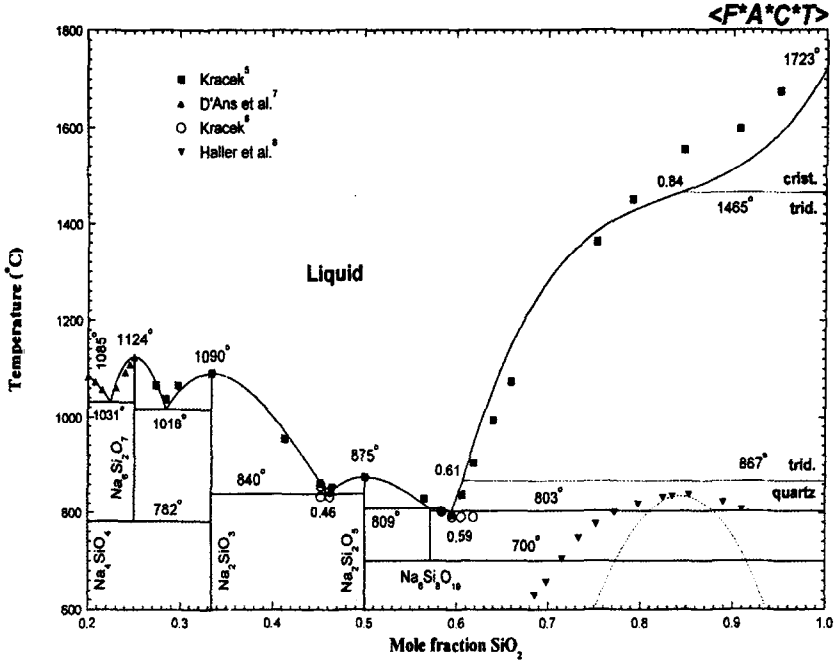

Figure 1: Optimized[4] $NaO_{0.5}$-SiO_2 phase diagram. Experimental points : ■[5] ○[6] ▲[7] ▼[8]

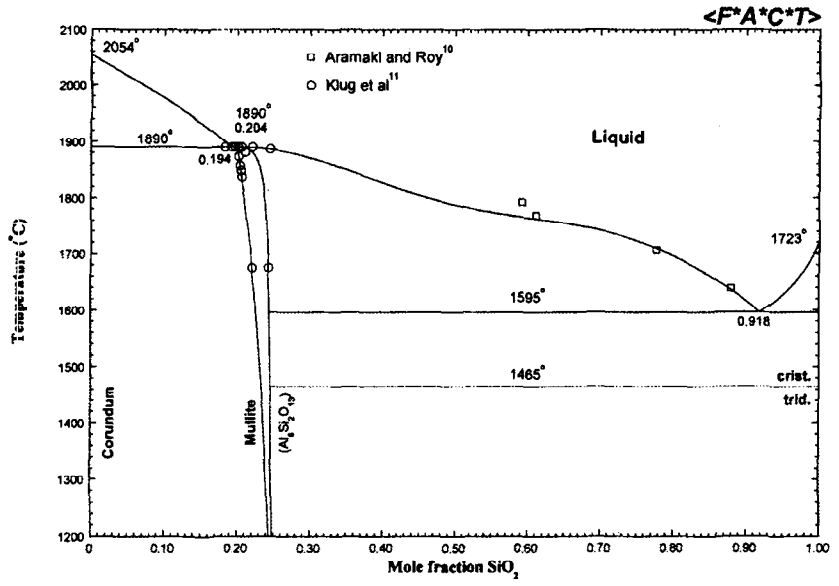

Figure 2: Optimized[9] $AlO_{1.5}$-SiO_2 phase diagram. Experimental points: □[10] ○[11]

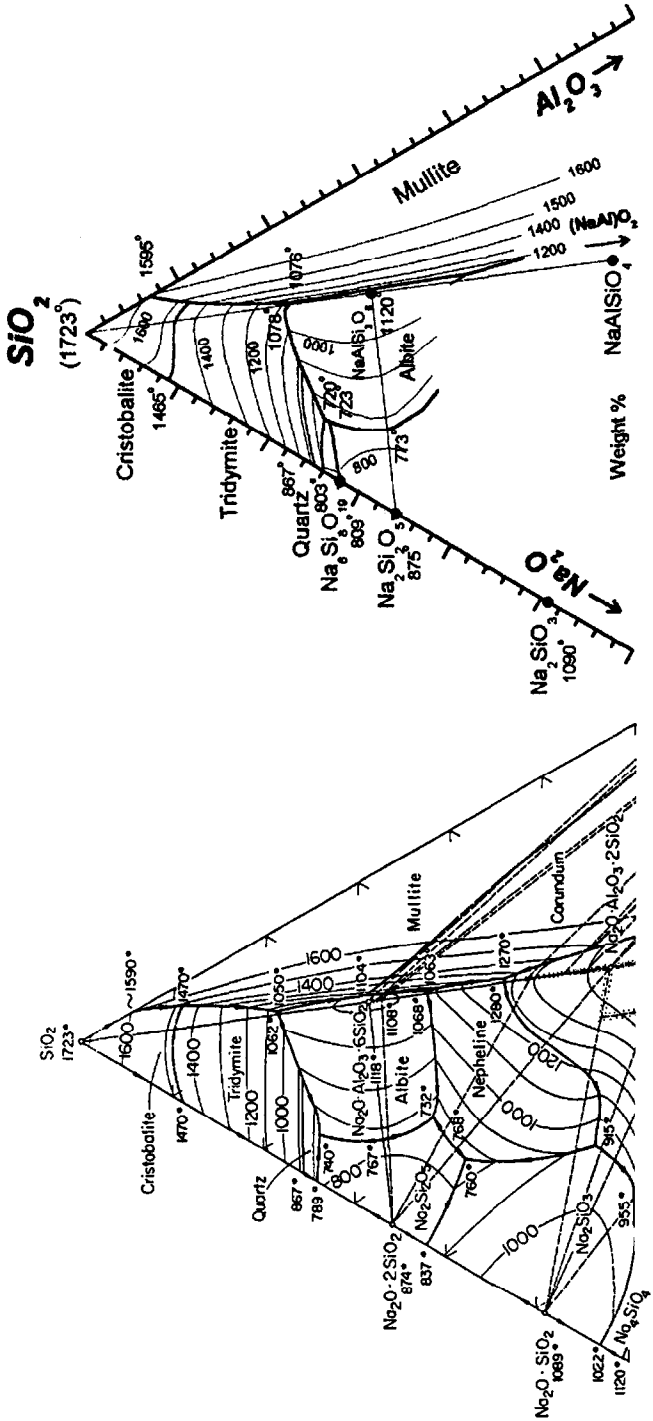

Figure 3: Liquidus surface of the Na_2O-Al_2O_3-SiO_2 system in the SiO_2-rich region: (a) as reported by Osborn and Muan[20]; (b) calculated. (composition in weight%; T in °C)

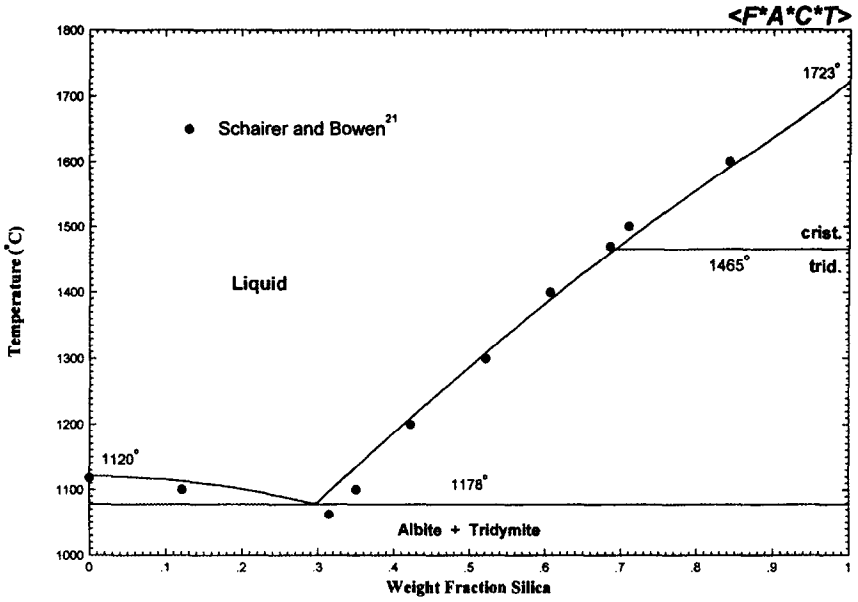

Figure 4: Calculated liquidus surface along the albite ($NaAlSi_3O_8$) – silica (SiO_2) join compared to experimental data[21]

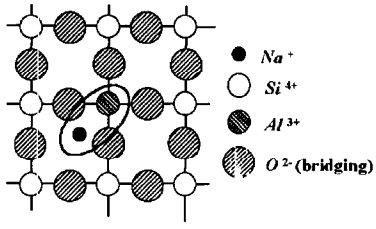

Figure 5: A simplified two-dimensional representation of the charge compensation effect in SiO_2-rich Na_2O-Al_2O_3-SiO_2 melts.

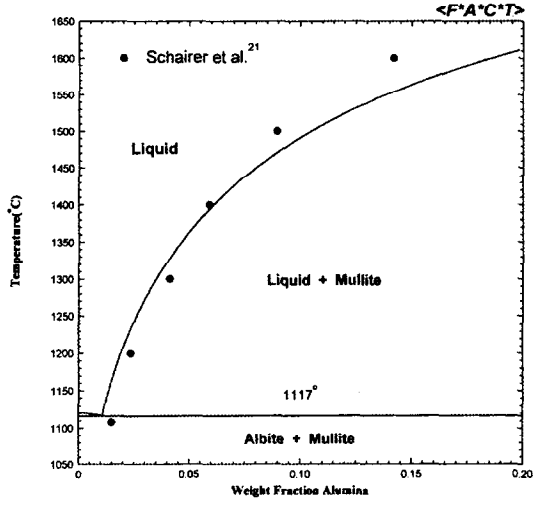

Figure 6: Calculated liquidus surface along the albite ($NaAlSi_3O_8$) – alumina (Al_2O_3) join compared to experimental data[21]

2-2. The K_2O-Al_2O_3-SiO_2 system

The K_2O-Al_2O_3-SiO_2 system was also optimized with the same model. Experimental [20] and calculated ternary liquidus surfaces are compared in Fig. 7. The optimization of the binary K_2O-SiO_2 system was reported previously [4] along with values of the standard Gibbs energies of K_2O and of the binary compounds. Standard Gibbs energies of the ternary compounds leucite ($KAlSi_2O_6$) and feldspar ($KAlSi_3O_8$), taken from the literature [22, 24], are compiled in Table 1. The value of S^o_{298} of leucite was adjusted by 15.834 J/mol in the present optimization. The parameters Δg^o_{KAl}, $\Delta g^o_{(KAl)K}$ and $\Delta g^o_{(KAl)Al}$ were all set to zero. Optimized expressions were obtained for $\Delta G^o_{(KAl)O_2}$ and $\Delta g^o_{(KAl)Si}$:

$$\Delta G^o_{(KAl)O_2} = -167360 \quad J/mol \tag{18}$$

$$\begin{aligned}\Delta g^o_{(KAl)Si} = &-37681+26.397T+63153Y_{Si}\\ &+\left(21916-25.104\,T\right)\left(Y_{Al}/\left(Y_K+Y_{Al}+Y_{(KAl)}\right)\right)\\ &-7950\left(Y_K/\left(Y_K+Y_{Al}+Y_{(KAl)}\right)\right) \quad J/mol\end{aligned} \tag{19}$$

The expression for $\Delta g^o_{(KAl)Si}$ contains two ternary parameters for the $(KAl)O_2$-$AlO_{3/2}$-SiO_2 "sub-system" and one ternary parameter for the SiO_2-$(KAl)O_2$-$KO_{1/2}$ "sub-system".

2-3. The Na_2O-K_2O-Al_2O_3-SiO_2 system

The liquidus surface of the SiO_2-$NaAlSiO_4$-$KAlSiO_4$ system, as reported by Schairer [25], is shown in Fig. 8a. This liquidus was calculated using the present model, whereby the liquid is treated as consisting of 6-components, $NaO_{1/2}$-$KO_{1/2}$-$AlO_{3/2}$-$(NaAl)O_2$-$(KAl)O_2$-SiO_2. No additional parameters were used for the liquid. The denominators of the ternary terms in Eqs (17, 19) were set to (Y_{Al} + Y_{Na} + Y_K + $Y_{(NaAl)}$ + $Y_{(KAl)}$) for interpolation into the multicomponent system. The solid solution of $KAlSi_2O_6$ (leucite) and $NaAlSi_2O_6$ (jadeite) was treated as ideal, with the standard Gibbs energy of jadeite, given in Table 1, taken from the literature [22, 23]. The solid solution of $NaAlSi_3O_8$ and $KAlSi_3O_8$ was treated as sub-regular, with the following optimized expression for the excess Gibbs energy :

$$g^E = X_{NaAlSi_3O_8}X_{KAlSi_3O_8}\left(5063+4.184T+6276X_{NaAlSi_3O_8}\right) \quad J/mol \tag{20}$$

The calculated liquidus surface in Fig. 8b is in good agreement with the measured liquidus.

3. CONCLUSIONS

In SiO_2-rich Na_2O-Al_2O_3-SiO_2 melts, a "charge compensation effect" occurs whereby the substitution of a trivalent Al^{3+} for a tetravalent Si^{4+} in the tetrahedral network is facilitated by association of the Al^{3+} with a Na^+ to form an $(NaAl)^{4+}$ associate. This effect has been successfully modeled by considering the $(NaAl)^{4+}$ associates as separate species in the melt which is then treated formally as a quaternary solution of the components $NaO_{1/2}$-$AlO_{3/2}$-$(NaAl)O_2$-SiO_2 in the quasichemical pair approximation. The liquidus surface at high SiO_2 contents is reproduced very well, with only a few parameters.

Good agreement has also been obtained for the K_2O-Al_2O_3-SiO_2 and Na_2O-K_2O-Al_2O_3-SiO_2 liquidus surfaces at high SiO_2 contents.

The model is only applicable at molar ratios Si/(Na+K+Al) greater than about 0.6. As the SiO_2 content is decreased below this value, the network structure progressively breaks down, and it becomes easier for alumina to enter the solution even without charge compensation. It may be possible to extend the model to lower SiO_2 contents by permitting the Gibbs energy of formation of $(NaAl)O_2$, $\Delta G^o_{(NaAlO_2)}$, to vary with X_{SiO_2}, becoming less negative as X_{SiO_2} decreases.

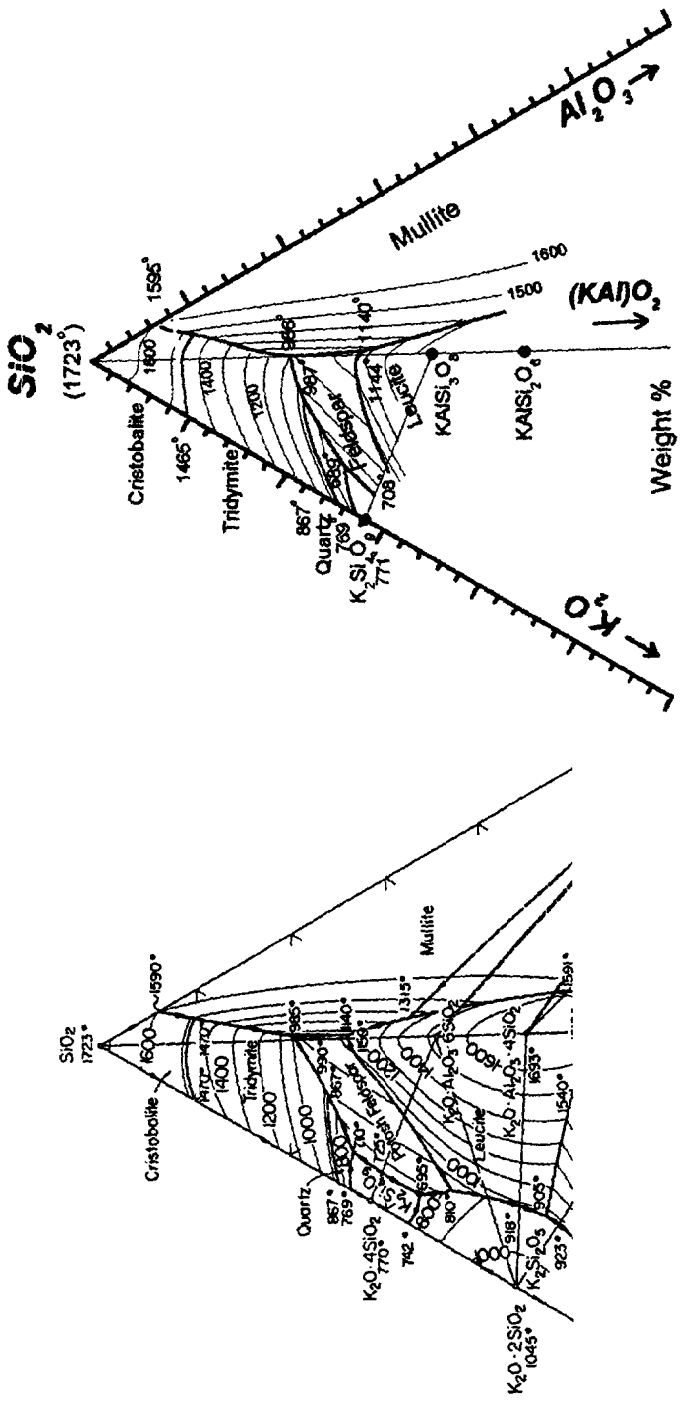

Figure 7: Liquidus surface of the K_2O-Al_2O_3-SiO_2 system in the SiO_2-rich region: (a) as reported by Osborn and Muan[20]; (b) calculated. (composition in weight%; T in °C).

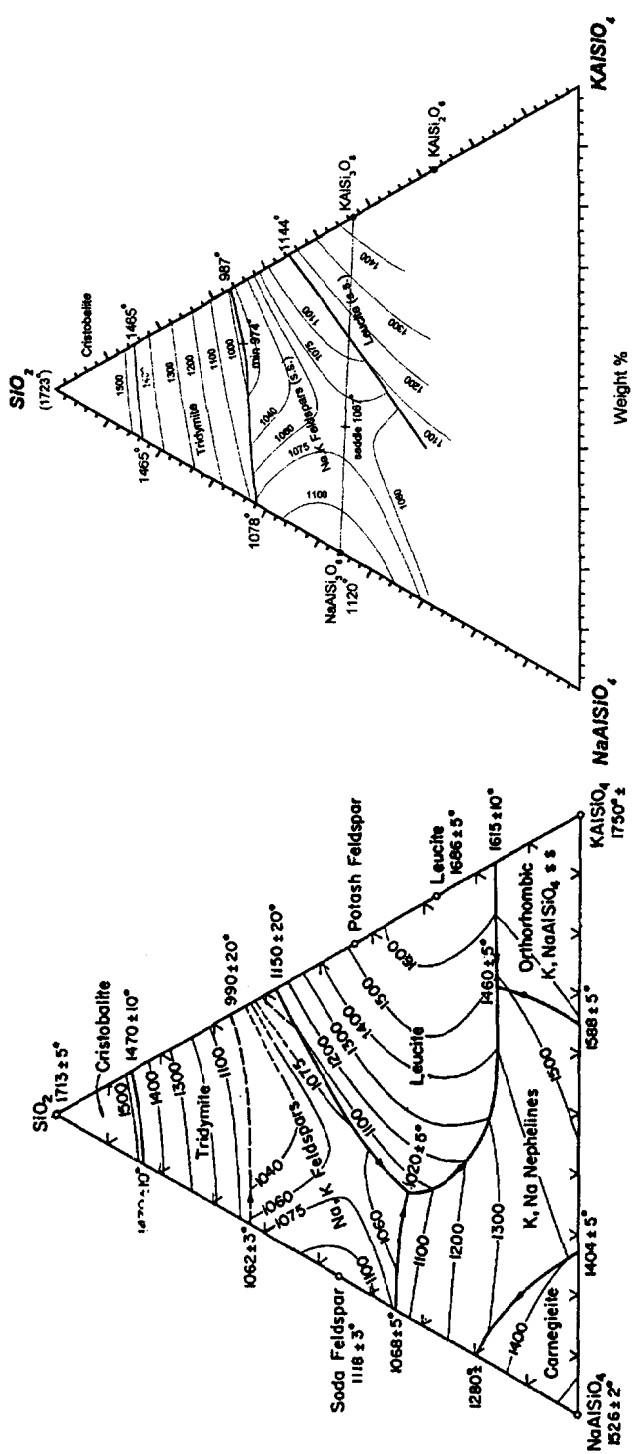

Figure 8: Liquidus surface of the $NaAlSiO_4$-$KAlSiO_4$-SiO_2 system : (a) as reported by Schairer[25]; (b) calculated. (composition in weight%; T in °C).

4. REFERENCES

1. A.D. Pelton and M. Blander, *Proc. AIME Symposium on Molten Salts and Slags, L. Tahoe, Nevada*, pp 281-294, TMS-AIME, Warrendale, PA (1984).

2. A.D. Pelton and M. Blander, *Metall. Trans.*, **17B**, 805-815 (1986).

3. M. Blander and A.D Pelton, *Geochim. et Cosmochim. Acta.*, **51**, 85-95 (1987).

4. P.Wu, G. Eriksson and A.D. Pelton, *J. Am. Ceram. Soc.*, **76**, 2059-64 (1993).

5. F.C. Kracek, *J. Phys. Chem.*, **34**, 1583-98 (1930).

6. F.C. Kracek, *J. Am. Chem. Soc.*,**61**, 2863-77 (1939).

7. J.D'Ans and J. Loeffler, *Z. Anorg. Allg. Chem.*, **191**, 1-34 (1930).

8. W. Haller, D. M. Blackburn and J. M. Simmons, *J. Am. Ceram. Soc.*, **57**, 120-126 (1974).

9. G. Eriksson and, A.D. Pelton, *Metall. Trans.*, **24B**, 807-816 (1993).

10. S. Aramaki and R. Roy, *J. Am. Ceram. Soc.*, **45**, 229-42 (1962).

11. F.J. Klug. S. Prochazka, and R.H. Doremus, *J. Am. Ceram. Soc.*, **70**, 750-59 (1987).

12. P. Wu, "Optimization and Calculation of Thermodynamic Properties and Phase Diagrams of Multicomponent Oxide Systems", Ph.D. thesis, Ecole Polytechnique, Montreal (1992).

13. P. Wu, G. Eriksson, A.D. Pelton and M. Blander, *Iron and Steel Inst. of Japan Journal*, **33**, 25-34 (1993).

14. S. Degterov and A.D. Pelton, *J. Phase Equilibria*, **17**, 488-494 (1996).

15. D. Degterov and A.D. Pelton, *J. Phase Equilibria*, **17**, 476-87 (1996).

16. S. Degterov and A.D. Pelton, *Metall. and Mat. Trans.*, **28B**, 235-42 (1997).

17. E. Jak, S. Degterov, P.C. Hayes and A.D. Pelton, *Fuel*, **77**, 77-84 (1997).

18. E. Jak, S. Degterov, P. Wu., P. Hayes and A.D. Pelton, *Metall. and Mat. Trans.*, ***28B***, 1011-18 (1998).

19. E. Jak, S. Degterov, P. Hayes and A.D. Pelton, *Canad. Metall. Quart.*, **37**, 41-47 (1998).

20. E.F. Osborn and A. Muan, *Phase Equilibrium Diagrams of Oxide Systems*, The American Ceramic Society and the Edward Orton Jr. Ceramic Foundation, Columbus, Ohio (1960).

21. J.F. Schairer and N L. Bowen, *Am. J. Sci.*, **254**, 163 (1956).

22. R.G. Berman and T.H. Brown, *Contrib. Miner. Petrol.*, **89**, 168-83 (1985).

23. S.K. Saxena, N. Chatterjee, Y. Fei and G. Shen, *Thermodynamic Data on Oxides and Silicates*, Springer-Verlag, NY (1993).

24. R.A. Robie, B.S. Hemingway and J.R. Fisher, *Thermodynamic Properties of Minerals and Related Substances at 298.15 K and 1 Bar Pressure and at Higher Temperatures*, U.S. Gov't Printing Office, Washington, D.C. (1978).

25. J. F. Schairer, *J. Geol.*, **58**, 514 (1950).

ACKNOWLEDGEMENTS

This work was supported by the Natural Sciences and Engineering Research Council of Canada. A scholarship for P.C. from the "Fonds pour la formation de chercheurs et l'aide à la recherche (Fonds FCAR)" of Qu ebec is also gratefully acknowledged.

TABLE 1

Thermodynamic Properties Relative to Elements at 298.15 K

$$H\left(J\cdot mol^{-1}\right)=A+\int_{298.15}^{T} C_p\,dT$$

$$S\left(J\cdot mol^{-1}\cdot K^{-1}\right)=B+\int_{298.15}^{T}\left(C_p/T\right)dT$$

$$C_p\left(J\cdot mol^{-1}\cdot K^{-1}\right)=a+b\left(10^{-3}\right)T+c\left(10^{5}\right)T^{-2}+dT^{-1/2}+e\left(10^{-8}\right)T^{-3}+f\left(10^{-6}\right)T^{2}$$

		A	B	a	b	c	d	e	f	Ref
$NaAlSi_3O_8$ (albite)	298-1391 K	-3919526.2	224.41200	393.63574		-78.92823	-2415.5000	10.706360		22,23
$NaAlSi_2O_6$ (jadeite)	298-1300 K	-3025118.2	133.57395	311.29297		-53.50264	-2005.1010	6.625669		22,23
$KAlSi_2O_6$ (feldspar)	298-1436 K	-3970790.8	214.14511	664.35523	-157.33000	-84.16546	-6772.4199	18.364255	34.769000	22
	1436-1473 K	-3959703.9	229.15691	381.37231		-120.37252	-1941.0450	18.364255		22
$KAlSi_2O_6$ (leucite)	298-1966 K	-3029541.9	195.86222*	271.14000		-78.57200	-944.1000	9.592000		22,24 * this work